
Sequential Model for Predicting Patient Adherence in Subcutaneous Immunotherapy for Allergic Rhinitis

Yin Li^{1*}, Yu Xiong^{2*}, Wenxin Fan³, Kai Wang¹, Qingqing Yu¹, Liping Si⁴, Patrick van der Smagt^{5,6}, Jun Tang^{1*} and Nutan Chen⁶

¹ Department of Otorhinolaryngology, The First People's Hospital of Foshan, China

² Department of Otorhinolaryngology, The Second Affiliated Hospital of Guizhou University of Traditional Chinese Medicine, Guiyang, China

³ Chinese Academy of Sciences Shenzhen Institutes of Advanced Technology, Shenzhen, China

⁴ Department of Radiology, Zhongshan Hospital, Fudan University, Shanghai, China

⁵ ELTE University, Budapest, Hungary

⁶ Machine Learning Research Lab, Volkswagen Group, Munich, Germany

Correspondence*:

Jun Tang

fsyyytj@126.com

ABSTRACT

Objective: Subcutaneous Immunotherapy (SCIT) is the long-lasting causal treatment of allergic rhinitis. How to enhance the adherence of patients to maximize the benefit of allergen immunotherapy (AIT) plays a crucial role in the management of AIT. This study aims to leverage novel machine learning models to precisely predict the risk of non-adherence of patients and related systematic symptom scores, to provide a novel approach in the management of long-term AIT.

Methods: The research develops and analyzes two models, Sequential Latent Actor-Critic (SLAC) and Long Short-Term Memory (LSTM), evaluating them based on scoring and adherence prediction capabilities.

Results: Excluding the biased samples at the first time step, the predictive adherence accuracy of the SLAC models is from 60% to 72%, and for LSTM models, it is 66% to 84%, varying according to the time steps. The range of Root Mean Square Error (RMSE) for SLAC models is between 0.93 and 2.22, while for LSTM models it is between 1.09 and 1.77. Notably, these RMSEs are significantly lower than the random prediction error of 4.55.

Conclusion: We creatively apply sequential models in the long-term management of SCIT with promising accuracy in the prediction of SCIT nonadherence in Allergic Rhinitis (AR) patients. While LSTM outperforms SLAC in adherence prediction, SLAC excels in score prediction for patients undergoing SCIT for AR. The state-action-based SLAC adds flexibility, presenting a novel and effective approach for managing long-term AIT.

*These authors contributed equally to this work.

Keywords: Allergic rhinitis, Allergen immunotherapy, Adherence, Sequential model, Latent variable model

1 INTRODUCTION

Allergic rhinitis is characterized by allergen-specific IgE-mediated inflammation in upper respiratory inflammation with a prevalence of up to 30 % worldwide (Meltzer, 2016). In addition to allergen avoidance as the superior criterion, allergen-specific immunotherapy (AIT) aims to induce specific allergen immune tolerance, consequently achieving a status of clinical symptom remission. The repeatable intake of the specific unmodified or chemically modified allergens (allergoids) was the key to maintaining the symptoms. Among these approaches of AIT, subcutaneous immunotherapy (SCIT), sublingual immunotherapy (SLIT), and lymphatic immunotherapy (SLIT) are demonstrated as the mainstream treatments regarding efficacy, safety, and side effects. Compared to the SLIT, SCIT is a clinic-dependent treatment in which the patient accepted an allergen extract injection subcutaneously. It is divided into the initial treatment stage (dose accumulation stage) and the maintenance treatment stage (dose maintenance stage). The World Health Organization (WHO) recommends that immunotherapy be maintained for three to five years and clinically recommended for at least two years. Patient adherence is a critical factor in ensuring long-lasting efficacy and sustaining symptom-relieving effects.

Due to the long duration of SCIT, cumbersome process, slow onset, individual differences in treatment effect, and other factors fundamentally impact the completeness of therapeutics. From the reported studies on AIT, the rate of adherence ranged from around 25% to over 90% (Passalacqua et al., 2013). The WHO adopted the definition of ‘adherence’ as “the extent to which a person’s behavior, such as taking medication, following a diet, or executing lifestyle changes, corresponds with agreed recommendations from a health care provider” (Organization et al., 2003). In recent EAACI guidelines, it is highlighted to educate patients on how immunotherapy works and on explaining the importance of compliance to the regular doses for three years of treatment (Roberts et al., 2018).

The multiple approaches were introduced into the field of improving adherence and supervising patient outcomes with systematic and technological interventions to prevent incomplete discontinuation of the treatment. The intervention from a clinic in advance running through the whole treatment cycle was approved as an effective approach. In facing the multitude of personalized data from patients, how to precisely identify and assess the risk of upcoming non-adherent behavior, a clinical prediction model is promising in the application.

In healthcare, machine learning, especially sequential models, stands at the forefront of innovation, providing new ways to analyze complex medical data and improve patient treatments. These models excel in processing and analyzing time-dependent data, making them ideal for predicting patient adherence to treatments like SCIT for AIT. By effectively utilizing sequential data, these algorithms uncover hidden temporal patterns and correlations, leading to more accurate and personalized treatment plans. In this study, we have selected and evaluated two specific sequential models tailored to this scenario. Our findings demonstrate that these models are not only effective in predicting patient adherence to medical treatments but also invaluable in enhancing treatment strategies, thereby making a significant contribution to patient-centered healthcare.

2 RELATED WORK

Non-sequential models for adherence prediction. A hybrid model was presented to combine artificial neural networks (ANNs) and the genetic algorithm (GA) to examine 26 factors influencing adherence to dietary plans (Mousavi et al., 2022). Wang et al. (2020) developed two machine learning methods, neural network (NN) and support vector machine (SVM), to predict nonadherence in Crohn's Disease patients. These models assist caregivers by streamlining the intervention process using azathioprine (AZA). Warren et al. (2022) investigated the relationship between patient adherence to prescribed medication for opioid use disorder and various risk factors in patients with opioid use disorder. Four different machine learning classifiers were proposed, including Logistic Regression, Decision Tree, Random Forest, and XGBoost. They compared the performance of these classifiers to explore the association. Since the adherence threshold can determine the prediction model's performance by the binary adherence status, Ruff et al. (2019) proposed a simulation framework to assess the performance of prediction models based on different adherence thresholds.

Sequential models for adherence prediction. Hsu et al. (2022) investigated the advantages of incorporating patient history into the prediction of medication adherence. They assessed the performance of temporal deep learning models, particularly LSTM and simple Recurrent Neural Networks (RNN), and compared these with non-temporal models such as Multilayer Perceptrons (MLP), ridge classifiers, and logistic regression. To optimize the efficacy of cognitive training for older adults, Singh et al. (2022) employed multivariate time series analysis and developed personalized models for each patient to capture their unique adherence patterns. However, the sequential data of patients is often characterized by fluctuating adherence and high dropout rates, resulting in uneven, unaligned, and missing values in the time series data. To address this challenge, Schleicher et al. (2023) applied change point detection to identify phases with varying dropout rates, presented methods for handling uneven and misaligned time series, and utilized time series classification to predict the user's phase.

3 METHODS

In this section, we outline the comprehensive methodologies employed in our study. These methods are designed to rigorously analyze the effectiveness of SCIT in treating AR patients. We detail the study design, population criteria, treatment protocols, and sequential models to provide a clear understanding of our research framework.

3.1 Study design

The study design is a critical component that shapes the direction and reliability of our research. It includes a systematic approach to selecting the study population, the treatment methods applied, and the evaluation criteria.

3.1.1 Population

A retrospective analysis including 205 AR patients who started SCIT treatment between August 2018 and September 2019 in the Immunotherapy Center at the First People's Hospital of Foshan was performed. According to the Guidelines for the Diagnosis and Treatment of Allergic Rhinitis (2015 Edition), the recruit criteria were formulated: patients with skin index (SI) of skin prick test (SPT) ++ or above or specific Immunoglobulin E (sIgE) level in serum to Derp/Derf ≥ 0.35 kU/L which exposure to dust mites was confirmed as the major allergen by allergen tests, including: (1) Patients with mild to moderate asthma; (2)

Patients with moderate to severe persistent rhinitis; (3) Mild to moderate asthma with allergic rhinitis (and/or allergic conjunctivitis); (4) Patients with mild to moderate asthma and eczema. Exclusion criteria included: (1) severe or uncontrolled bronchial asthma with continuous monitoring of Forced Expiratory Volume in one second (FEV1) < 70% per of the expected value; (2) Patients with asthma whose symptoms or reduced lung function continue to fail to be controlled with grade 4 or 5 treatment; (3) Patients sensitized to other allergens such as pet furs, pollens or molds; (4) Patients who are taking beta-2 blockers or angiotensin-converting enzyme inhibitors; (5) Patients with serious underlying diseases, including cardiovascular and cerebrovascular diseases, autoimmune diseases and immunodeficiency diseases, malignant diseases, and chronic infectious diseases; (6) Patients with serious mental illness, lack of compliance, or inability to understand the risks and limitations of treatment; This study followed the tenets of the Declaration of Helsinki and was approved by the Ethics Committee of the First People's Hospital of Foshan, Foshan, China. Written informed consent was obtained from all of the study participants.

3.1.2 SCIT treatment and evaluation

Before administering SCIT to enrolled patients, they will first perform a routine physical examination, inquire about related information since the last injection (including allergy symptoms), and post-injection, patients are observed for 30 minutes in case of the occurrence of side effects. Standardized aluminum hydroxide adsorbed Derp allergen extracts (Allergopharma, Reinbeck, Germany) were used for SCIT. According to the manufacturer's instructions, in the dose accumulation phase with weekly injections of allergen extracts with a gradually increased concentration from 100 SQ-U/mL to 10,000 SQ-U/mL, respectively injected 0.2, 0.4, 0.8 mL; after reaching the maintenance dose, 100,000 standardized quality units was used. In the maintenance phase, an injection interval of 6 ± 2 weeks was carried out according to the manufacturer's recommendations.

Patients receive regular treatment evaluations, including symptom scores and medication scores. The symptom score recorded a total of nasal symptoms (nasal itching, sneezing, rhinorrhea, nasal congestion), ocular symptoms (ocular itching, lacrimation), and pulmonary symptoms (shortness of breath, tightness in chest, perennial cough, wheezing), and assessed symptom severity using the visual analogue scale (VAS). In the VAS score, the score of each symptom is from 0 to 10. 0 indicates that the patient has no discomfort and 10 indicates that the patient is very uncomfortable. The patient gives the score of each symptom according to the actual situation, and the sum of all symptom scores is the symptom score. Medication score recorded the use of current adjuvant medication within 1 month to reach symptom relief. The use of oral antihistamines, antileukotrienes, and bronchodilators were recorded as one point, local glucocorticoids as two points, oral glucocorticoids or combined medication (hormones and β_2 receptor agonists) as three points, and the total cumulative score was the medication score. Symptom scores and medication scores were assessed once at registration of SCIT and then thereafter.

Due to the separated injection regimen within 16 weeks and thereafter, all the chosen patients completed the four months of SCIT, we chose the fourth month as the starting point of the observation. According to our previous experience, one year after the start was the peak of the withdrawal, so we added a time point at 18 months to further assess and follow up on the related symptom score and individual status. The data collection spans six time steps: at 0, 4, 12, 18, 24, and 36 months. This approach is standard in medical treatment, although for optimal model performance, an equal distribution of time intervals would be preferable.

3.1.3 Data Collection

Data were collected from patient records in hospitals, and the following information was extracted for analysis: patient age, gender, distance to clinic, ratio of AIT cost to family income, allergen test results, etc., as well as patient VAS system score and medication score information, including baseline data of patients before injection therapy, adverse reactions to SCIT. For the descriptive analysis, categorical variables were given as numbers and percentages, and continuous variables were presented using mean, standard deviation, median, interquartile range (IQR), and minimum and maximum values.

3.1.4 Survey methods

Adherence was defined as the accomplishment of three years of AIT including the patients further received AIT. Non-adherence was defined as discontinuation of AIT at random time points during three years. The follow-up contents included (1) the main reasons for patients' discontinuation of treatment; (2) the duration of discontinuation of treatment, and (3) Allergic symptoms after discontinuation of treatment.

3.2 Sequential models

The focus of our study is the development of sequential models that can efficiently and accurately predict the progression of symptoms and adherence in patients undergoing SCIT. This involves a comprehensive analysis of the data collected, structured to provide insights into the treatment's effectiveness and patient compliance over time. Additionally, we explore and compare two distinct sequential models.

3.2.1 Data

| variables | | total | patients adherent | non-adherent |
|------------------------|--------|---------------|----------------------|--------------|
| age | ≤ 12 | 96 (46.7) | 40 | 56 |
| | 13–17 | 30 (14.6) | 10 | 20 |
| | ≥ 18 | 79 (38.7) | 23 | 56 |
| gender | Female | 62 (30) | 22 | 40 |
| | Male | 143 (70) | 51 | 92 |
| distance to clinic(km) | ≤ 10 | 136 (66) | 56 | 80 |
| | > 10 | 69 (34) | 17 | 52 |
| cost/family income(%) | < 30 | 107 (52.4) | 37 | 70 |
| | 30–50 | 77 (37.4) | 32 | 45 |
| | > 50 | 21 (10.2) | 4 | 17 |
| EOS($\times 10^9/L$) | | 0.37; 0.41 | 0.36; 0.52 | 0.38; 0.36 |
| EOS % | | 0.05; 0.04 | 0.05; 0.05 | 0.05; 0.05 |
| $\Delta NR(\%)$ | | 16.67; 59.70 | 30.00; 92.80 | 14.80; 50.00 |
| $\Delta PNIF(\%)$ | | 11.90; 34.50 | 12.70; 39.30 | 11.10; 28.80 |
| total IgE (kU/L) | | 286; 543 | 340; 487 | 226; 555 |
| sIgE of Derp (kU/L) | | 30.80; 68.480 | 31.30; 74.40 | 30.40; 67.80 |
| sIgE of Derf (kU/L) | | 40.00; 68.20 | 40.60; 75.10 | 37.10; 65.70 |
| Derp SPT SI | | 1.04; 0.58 | 1.00; 0.59 | 0.82; 0.55 |
| Derf SPT SI | | 1.00; 0.50 | 0.82; 0.51 | 0.80; 0.45 |

Table 1. Demographic and clinical data of the patients under subcutaneous immunotherapy. In the rows from Age to Cost/Family income, values indicate the number of patients (percentage, if available). Other rows represent the median and IQR. P-values are omitted due to their large values.

| reasons for SCIT withdrawal | number of non-adherent patients | | | | total by reason |
|-----------------------------|---------------------------------|------------|------------|------------|-----------------|
| | 5–12 mths | 13–18 mths | 19–24 mths | 25–36 mths | |
| no clinical improvement | 18 | 11 | 8 | 21 | 58 |
| medical issue | 3 | 1 | 2 | 0 | 6 |
| improved efficacy | 0 | 0 | 0 | 24 | 24 |
| schooling | 3 | 3 | 0 | 5 | 11 |
| side effects | 2 | 1 | 1 | 2 | 6 |
| Covid-19 | 9 | 7 | 3 | 1 | 20 |
| personal issue | 0 | 3 | 0 | 4 | 7 |
| total by time period | 35 | 26 | 14 | 57 | 132 |

Table 2. Detailed reasons for withdrawal from SCIT at different time points.

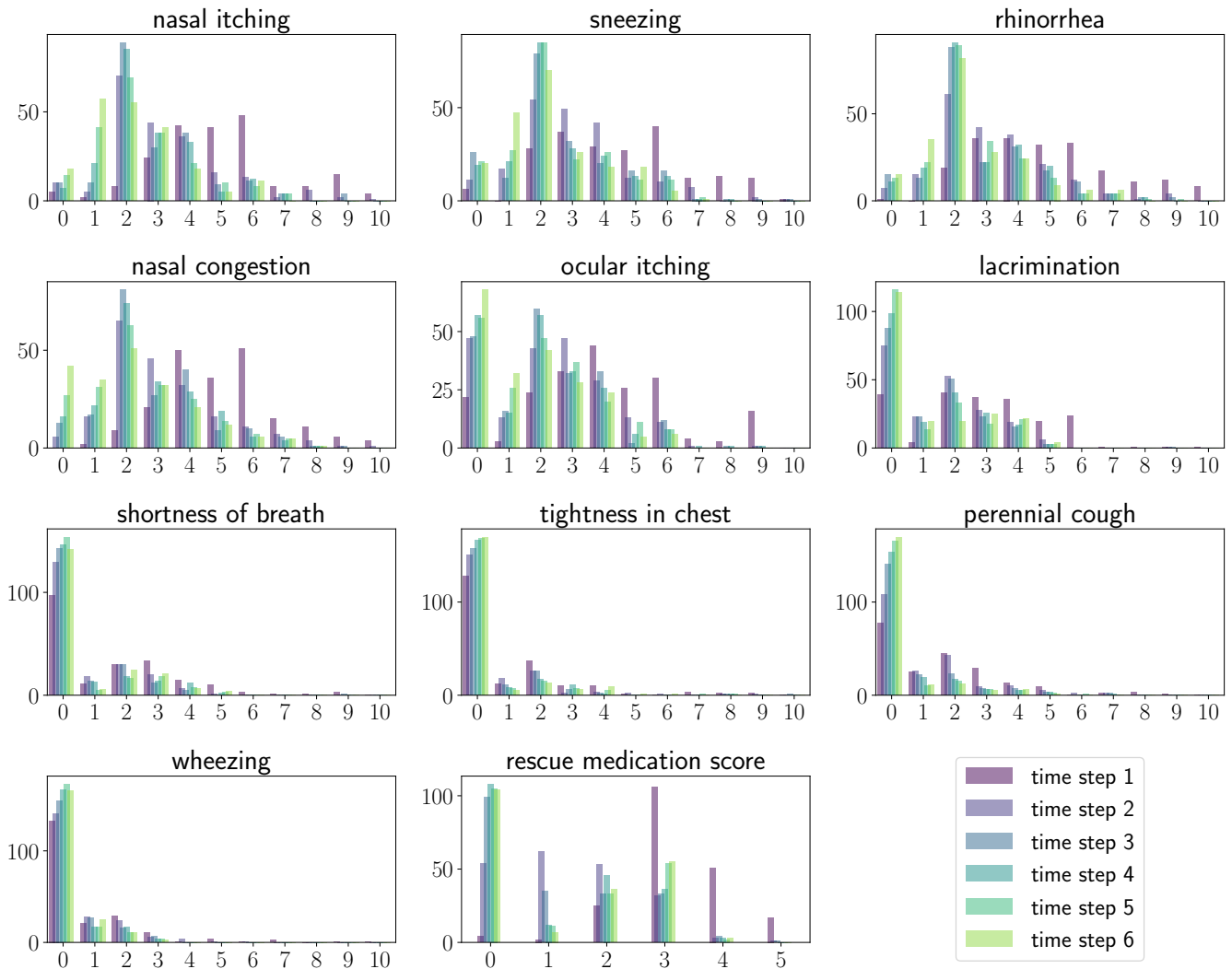


Figure 1. Histogram of scores across six-time steps. Score value (horizontal axis) vs. count (vertical axis).

We have a dataset D , comprising sequences $x_1, \dots, x_T \in R^{11}$, $y_1, \dots, y_{T-1} \in R^1$, and a corresponding action $a_t \in R^1$. In the context of healthcare, the observations encompass y_t (see Table 2) whether the patient will cease the treatment in the interval between the scoring measurements at x_t and x_{t+1} . The actions a_t represent the ongoing medical procedures for the patient during the period from x_t to x_{t+1} (see

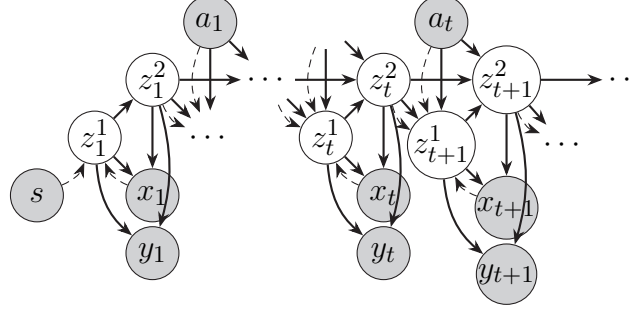


Figure 2. SLAC model schematic. Solid and dashed lines denote the generative and inference model pathways, respectively. The gray circles represent observed data, and the white circles denote latent variables. The figure is adapted from (Lee et al., 2020).

Fig. 1). In this context, a_t is binary, reflecting whether treatment is given, and is numerically equivalent to the adherence variable y_t . Despite their numerical equivalence, we maintain a distinction between action a_t and adherence y_t to enhance model clarity and accommodate future research expansions, potentially allowing for a wider range of action values. For each patient, we possess basic information $s \in R^{14}$ which includes age, gender, commute distance to clinic, ratio of cost to family income, eosinophils count, eosinophils percentage, nasal allergen provocation test (change of nasal resistance, $\Delta NR(\%)$), peak nasal inspiratory flow. $\Delta PNIF(\%)$), serum total IgE level, sIgE of *Dermatophagoides pteronyssinus* (Derp), sIgE of *Dermatophagoides farinae* (Derf), skin prick test (Derp, Derf) (see Table 1 for more details).

3.2.2 Sequential latent variable models

In our research, we employ the Stochastic Latent Actor-Critic (SLAC) model (Lee et al., 2020). However, our application differs from the original use of SLAC which is typically associated with reinforcement learning. Instead, we leverage its sequential latent-variable model without Actor-Critic. This approach aligns with similar methodologies found in other works (Krishnan et al., 2015; Karl et al., 2016; Gregor et al., 2018). The choice of the SLAC model was motivated by its ability to facilitate more efficient learning and superior generalization in intricate environments.

The sequential latent variable model consists of an inference model and a generative model (see Fig. 2). The inference model in a sequential latent variable model typically aims to approximate the posterior distribution of the latent variables given the observed data. It tries to infer the hidden states z based on the observed inputs x and some internal state s . The inference models the probability distributions of the latent variables z^1 and z^2 at different time steps. q_ϕ denotes the variational distribution parameterized by ϕ ,

$$z_1^1 \sim q_\phi(z_1^1 | x_1, s) \quad (1)$$

$$z_1^2 \sim p_\phi(z_1^2 | z_1^1) \quad (2)$$

$$z_{t+1}^1 \sim q_\phi(z_{t+1}^1 | x_{t+1}, z_t^2, a_t) \quad (3)$$

$$z_{t+1}^2 \sim p_\phi(z_{t+1}^2 | z_{t+1}^1, z_t^2, a_t). \quad (4)$$

The generative model, on the other hand, describes how the observed data is generated from the latent variables. It defines a process by which the latent states z give rise to the observations x . The generative model is described by a set of equations that represent the probability distributions of both the initial latent states and their transitions over time, as well as the likelihood of the observations given the latent states,

with p_ϕ indicating the parameterized generative distribution.

$$z_1^1 \sim p(z_1^1) \quad (5)$$

$$z_1^2 \sim p_\phi(z_1^2|z_1^1) \quad (6)$$

$$z_{t+1}^1 \sim p_\phi(z_{t+1}^1|z_t^2, a_t) \quad (7)$$

$$z_{t+1}^2 \sim p_\phi(z_{t+1}^2|z_{t+1}^1, z_t^2, a_t) \quad (8)$$

$$x_t \sim p_\phi(x_t|z_t^1, z_t^2) \quad (9)$$

$$y_t \sim p_\phi(y_t|z_t^1, z_t^2). \quad (10)$$

We have the evidence lower bound (ELBO):

$$\log p_\phi(x_{1:t+1}|a_{1:t}) \geq \left[\mathbb{E}_{(x_{1:T}, a_{1:T-1}) \sim D} \left[\mathbb{E}_{z_{1:T} \sim q_\phi} \sum_{t=0}^{T-1} \left(\log p_\phi(x_{t+1}|z_{t+1}) \right. \right. \right. \quad (11)$$

$$\left. \left. \left. - D_{KL}(q_\phi(z_{t+1}|x_{t+1}, z_t, a_t) \| p_\phi(z_{t+1}|z_t, a_t)) \right) \right] \right].$$

For ease of notation, we have $q(z_1|x_1, z_0, a_0) := q(z_1|x_1, s)$ and $p(z_1|z_0, a_0) := p(z_1)$. The ELBO provides a lower bound to the log-likelihood of the observed data, which is computationally intractable to compute directly. It is composed of two terms: the expected log-likelihood of the observed data given the latent variables, and the Kullback-Leibler (KL) divergence between the variational distribution and the prior distribution of the latent variables. Minimizing the KL divergence can be interpreted as enforcing the variational distribution to be as close as possible to the prior, while maximizing the expected log-likelihood ensures that the model accurately captures the distribution of the observed data. To predict the adherence, we have $\log p_\phi(y_{t+1}|z_{t+1})$ as a regulariser in the loss function.

The objective is to compute the parameters ϕ that minimize the KL divergence between the variational and prior distributions of the latent variables, subject to certain constraints. These constraints are related to the expected log-likelihood of the data under the model and are represented by the inequalities with thresholds ξ . These thresholds ensure that while minimizing the losses, the model also satisfies a minimum standard for score prediction and adherence classification performances.

Latent variable models, such as Variational Autoencoders (VAEs) (Kingma and Welling, 2014; Rezende et al., 2014) and their variants (e.g., SLAC), often encounter challenges (Sønderby et al., 2016; Kingma et al., 2016). Furthermore, a higher ELBO does not always lead to enhanced predictive performance, as discussed by Alemi et al. (2018); Higgins et al. (2017). However, the integration of scheduling strategies inspired by constrained optimization methods has been shown to significantly improve the training of latent variable models (Rezende and Viola, 2018; Klushyn et al., 2019). Consequently, we formulate the training

of our model into an optimization problem

$$\min_{\phi} \mathbb{E}_{(x_{1:T}, a_{1:T-1}) \sim D} \left[\sum_{t=0}^{T-1} [D_{KL}(q_{\phi}(z_{t+1}|x_{t+1}, z_t, a_t) || p_{\phi}(z_{t+1}|z_t, a_t))] \right] \quad (12)$$

$$\text{s.t.} \quad \mathbb{E}_{(x_{1:T}, a_{1:T-1}) \sim D} \left[\mathbb{E}_{z_{1:T} \sim q_{\phi}} \left[\sum_{t=0}^{T-1} -\log p_{\phi}(x_{t+1}|z_{t+1}) \right] \right] \leq \xi_{\text{score}} \quad (13)$$

$$\mathbb{E}_{(x_{1:T}, a_{1:T-1}, y_{1:T-1}) \sim D} \left[\mathbb{E}_{z_{1:T} \sim q_{\phi}} \left[\sum_{t=0}^{T-2} -\log p_{\phi}(y_{t+1}|z_{t+1}) \right] \right] \leq \xi_{\text{adherence}} \quad (14)$$

where in Eq. (13) we have regression with Gaussian distribution, and in Eq. (14) we use cross-binary entropy loss for classification. To solve the optimization problem, we incorporate the constraints into the objective function using Lagrange multipliers λ . We apply methods from (Chen et al., 2022) to adapt λ . This allows the model to balance the importance of the constraints relative to the divergence terms, which can help in avoiding common pitfalls in training such as suboptimal local minima and posterior collapse.

To avoid over-fitting, we incorporate dropout (Srivastava et al., 2014) and Mixup (Zhang et al., 2017). Subsequent research has extended the application of Mixup to latent variable models, specifically within the latent space (e.g., (Chen et al., 2020)). However, considering our need for data augmentation across all data dimensions, not limited to latent variables, we have selected to implement the original Mixup method in our experiments.

3.2.3 LSTM

Long short-term memory (LSTM) is a classical sequential model (Hochreiter and Schmidhuber, 1997). The primary objective of this study is to forecast y_t utilizing historical data, formulated as $y_t = f(x_{1:t}, y_{1:t-1}, s)$. To align this approach with the SLAC model for score prediction, an additional term x_{t+1} is also predicted,

$$(x_{t+1}, y_t) = f(x_{1:t}, y_{1:t-1}, s) \quad (15)$$

where f is a function represented by LSTM. The loss consists of cross entropy for adherence classification and Normalized Mean Squared Error Loss (NMSE) for score prediction.

In our scenarios, SLAC stands out due to its inherent flexibility over traditional sequential models like LSTM. This flexibility is primarily observed in its predictive capabilities. SLAC can predict y_t and use this prediction to influence the subsequent x_{t+1} . In contrast, LSTM only predicts a pair of y_t and x_{t+1} simultaneously, implying that we cannot use y_t to alter x_{t+1} . Although it is possible to modify the LSTM model to predict a pair of y_t and x_t , this approach encounters a similar issue for y_t : it cannot predict y_t using the information from x_t .

4 RESULTS

A total of 205 patients were enrolled in this study. The mean age was 17.57 ± 11.68 years, children and adolescents represented the major population (61.3 %) in AIT treatment. Males (70 %) were predominantly high in our cohort. The population with a commute distance to the clinic within 10 km was 66 percent. Due to a great portion of juveniles from the cohort, the ratio of cost to family income instead of personal

income was evaluated. The patients who undertook AIT cost less than 30% of monthly family income and account for half the distribution of the population, while 12.9% non-adherent patients undertook the 50% financial burden in AIT treatment.

The change of nasal resistance (NR) and peak nasal inspiratory flow (PNIF) after nasal allergen provocation (NPT) was used to evaluate the severity of symptoms by combining the symptom score. The change of NR after NPT from the adherent group was higher than the non-adherent group (30 % vs 14.8 %). The laboratory tests such as total IgE, sIgE of Derp and Derf, and SPT did not exhibit a significant difference between the two groups. For detailed characteristics of patients see Table 1.

The observed total non-adherence rate at the end of three years was 35.4% and the median of the SCIT duration was 18 months in the study. The rate of dropout in the third year(43.0%) was highest in comparison to the end of the first year (26.5 %) and the second year (30.0 %). The reason for the withdrawal from the patients included the concern of COVID-19, especially at the beginning of 2020 accounting for a 25 % portion of the non-adherent patients in the first year. The most influential reason for the withdrawal was unmet expectations for clinical improvement (43.9%). Medical issues including pregnancy status during the treatment period and other physical disorders were collected from patients leading to the withdrawal of SCIT (4.5 %). The significantly improved symptoms contributed to the reason for dropout, especially after two years SCIT treatments (18.2 %). The recorded cases from side effects accounted for 4.5 %, comprising the local and systematic adverse reactions (see Table 2).

We have a total of 205 samples, which we have randomly divided into a test dataset comprising 20 %, i.e., 41 samples. For our analysis, we employ a five-fold cross-validation approach. Additionally, we apply zero-mean and unit standard deviation (STD) normalization to the variables x and s .

The Root Mean Square Error (RMSE) metric is used to evaluate the precision of our medical score predictions. Furthermore, to assess the adherence predictions, we utilize a comprehensive set of metrics including accuracy, precision, recall, and the F1 score, each offering a unique perspective on the performance of our predictive models. Most of the figures in this study are presented using boxplots.

The uncertainties for both models are calculated using five-fold cross-validation. In addition, as SLAC is a probabilistic model, we also perform 100 samples from the latent space to compute its uncertainty.

4.1 One-Step Prediction

| metric | model | time step 1 | time step 2 | time step 3 | time step 4 | time step 5 |
|-----------|-------|--------------------|--------------------|--------------------|--------------------|--------------------|
| accuracy | LSTM | 1.00 ± 0.00 | 0.66 ± 0.03 | 0.80 ± 0.04 | 0.84 ± 0.05 | 0.74 ± 0.02 |
| | SLAC | 1.00 ± 0.01 | 0.70 ± 0.06 | 0.72 ± 0.04 | 0.71 ± 0.04 | 0.60 ± 0.06 |
| precision | LSTM | 1.00 ± 0.00 | 0.72 ± 0.01 | 0.86 ± 0.06 | 0.90 ± 0.05 | 0.62 ± 0.03 |
| | SLAC | 1.00 ± 0.00 | 0.75 ± 0.03 | 0.74 ± 0.03 | 0.71 ± 0.03 | 0.44 ± 0.05 |
| recall | LSTM | 1.00 ± 0.00 | 0.86 ± 0.06 | 0.83 ± 0.05 | 0.82 ± 0.08 | 0.61 ± 0.03 |
| | SLAC | 1.00 ± 0.01 | 0.87 ± 0.06 | 0.90 ± 0.03 | 0.86 ± 0.04 | 0.70 ± 0.10 |
| F1 score | LSTM | 1.00 ± 0.00 | 0.79 ± 0.03 | 0.84 ± 0.03 | 0.85 ± 0.05 | 0.62 ± 0.03 |
| | SLAC | 1.00 ± 0.00 | 0.81 ± 0.04 | 0.81 ± 0.02 | 0.78 ± 0.03 | 0.54 ± 0.06 |

Table 3. Comparison of LSTM and SLAC over different time steps. The results are expressed as a mean \pm standard deviation. The better results are highlighted in bold.

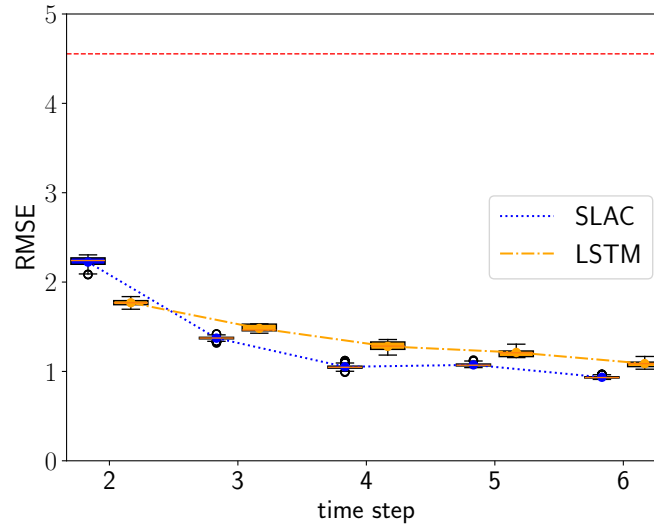


Figure 3. RMSE of the prediction step by step. The red dashed line is the RMSE of random prediction with Uniform distribution. See Fig. 5 and 6 for more details.

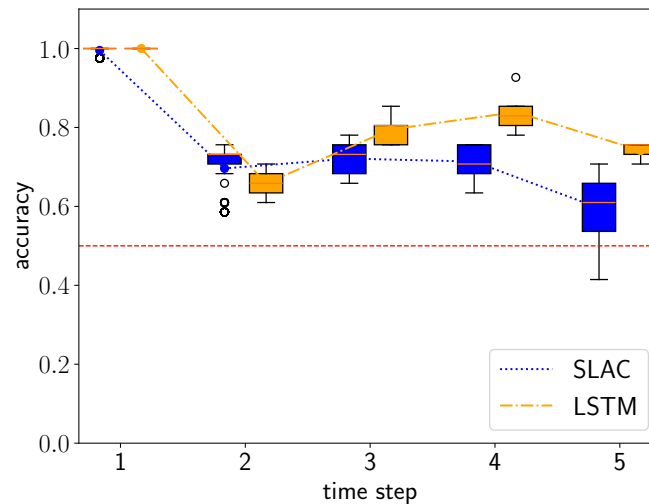


Figure 4. Accuracy of the prediction step by step. The red dashed line is the accuracy of random prediction with Uniform distribution. See Table 3 for more details.

In this experiment, our focus is on predicting the immediate next step. Within the SLAC, the prediction of y_t is based on the sequence $x_{1:t}$ and actions $a_{1:t-1}$. Additionally, we forecast the subsequent state x_{t+1} using the sequence $x_{1:t}$ along with actions $a_{1:t}$. In contrast, for LSTM, the predictions for both y_t and the next state x_{t+1} are derived from $x_{1:t}$ and $y_{1:t-1}$.

As illustrated in Fig.3, SLAC surpasses LSTM in performance beginning at time step two. The figure indicates that with an increased amount of historical data (additional time steps), SLAC achieves greater RMSE. Both SLAC and LSTM demonstrate considerably better over random prediction methods. Further insights are provided in Fig. 5 and Fig. 6, which provides detailed representations of each feature. In the prediction of specific local symptoms score, SLAC performs an improvement in error after step two with all parameters compared to LSTM. The results from RMSE in nasal and ocular symptoms display relatively high values compared to those for lower respiratory tract symptoms. This can be attributed to the fact that

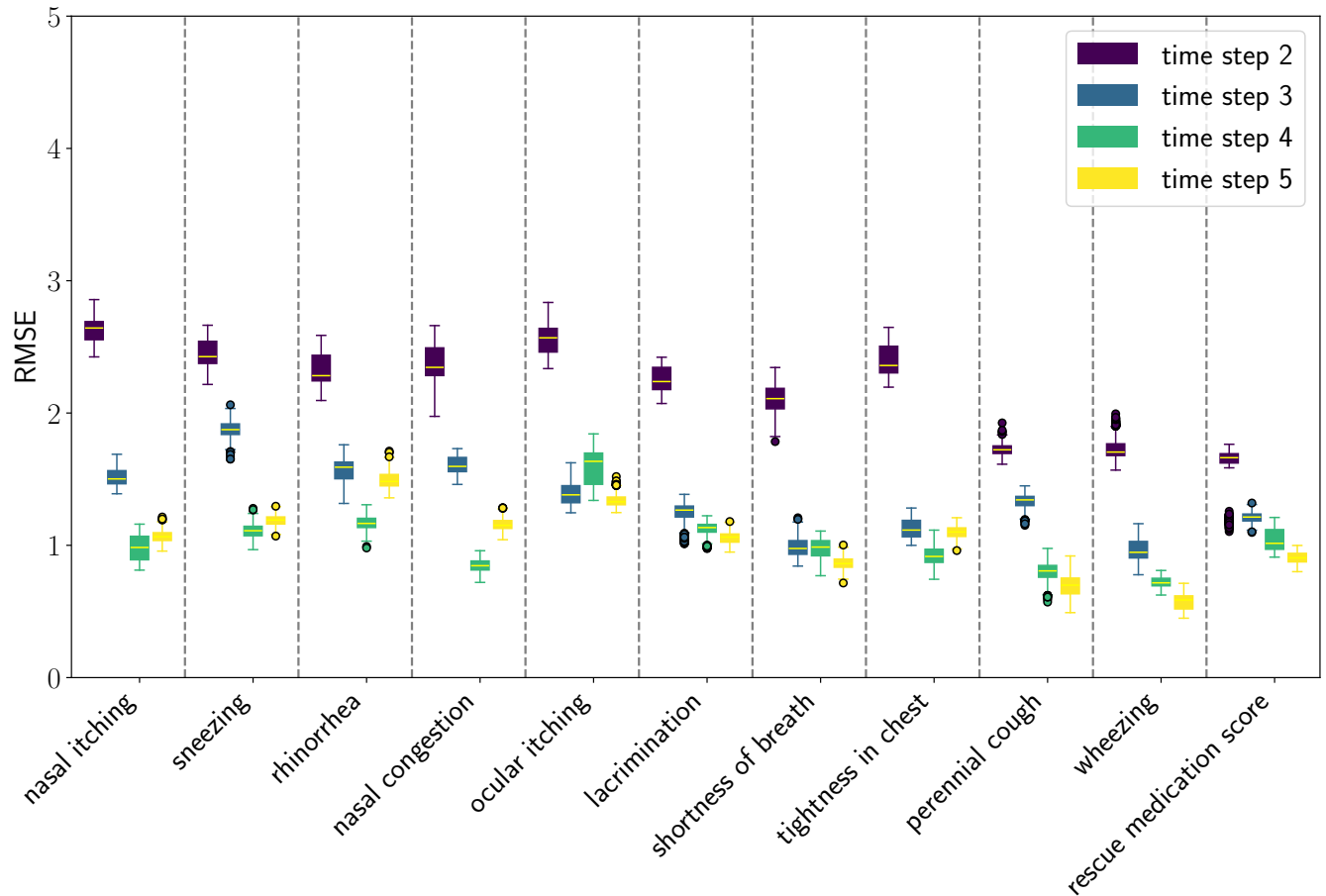


Figure 5. RMSE of SLAC one-step prediction across various scores and time steps.

the majority of patients in the cohort predominantly exhibited nasal and ocular symptoms, which presented a wide range of scores.

Fig. 4 demonstrates that from steps two to four, accuracy in adherence predictions improves with the inclusion of additional information. The first step exhibits a notable bias, as it only includes data from adherent patients, as detailed in Sec. 3.1.2. Nonetheless, both models adeptly manage this bias and achieve high-accuracy predictions. Prediction for the sixth step is not conducted due to the cessation of treatment by the hospital. In the fifth step, there is a decline in accuracy, likely due to the extended time interval of 12 months. Table 3 illustrates details of the classification for one-step prediction. Initially, both models exhibit perfect performance in Accuracy, Precision, and Recall at the first time step, but diverge in subsequent steps. In terms of Accuracy, LSTM generally outperforms SLAC, particularly evident at time steps three, four, and five. For Precision, LSTM again shows superior performance in the later time steps, except at time step two where SLAC marginally leads. However, in the Recall metric, SLAC surpasses LSTM from time step two onwards, indicating its strength in correctly identifying positive cases. The F1 score, which balances precision and recall, shows LSTM generally ahead, except at time step two where SLAC has a slight edge. This metric indicates LSTM's balanced capability in both precision and recall, especially in the later time steps. Overall, while both models start equally strong, LSTM demonstrates greater consistency and effectiveness across most metrics and time steps. SLAC, while lagging slightly behind in accuracy and precision, shows its robustness in recall, especially in the middle to later time steps.

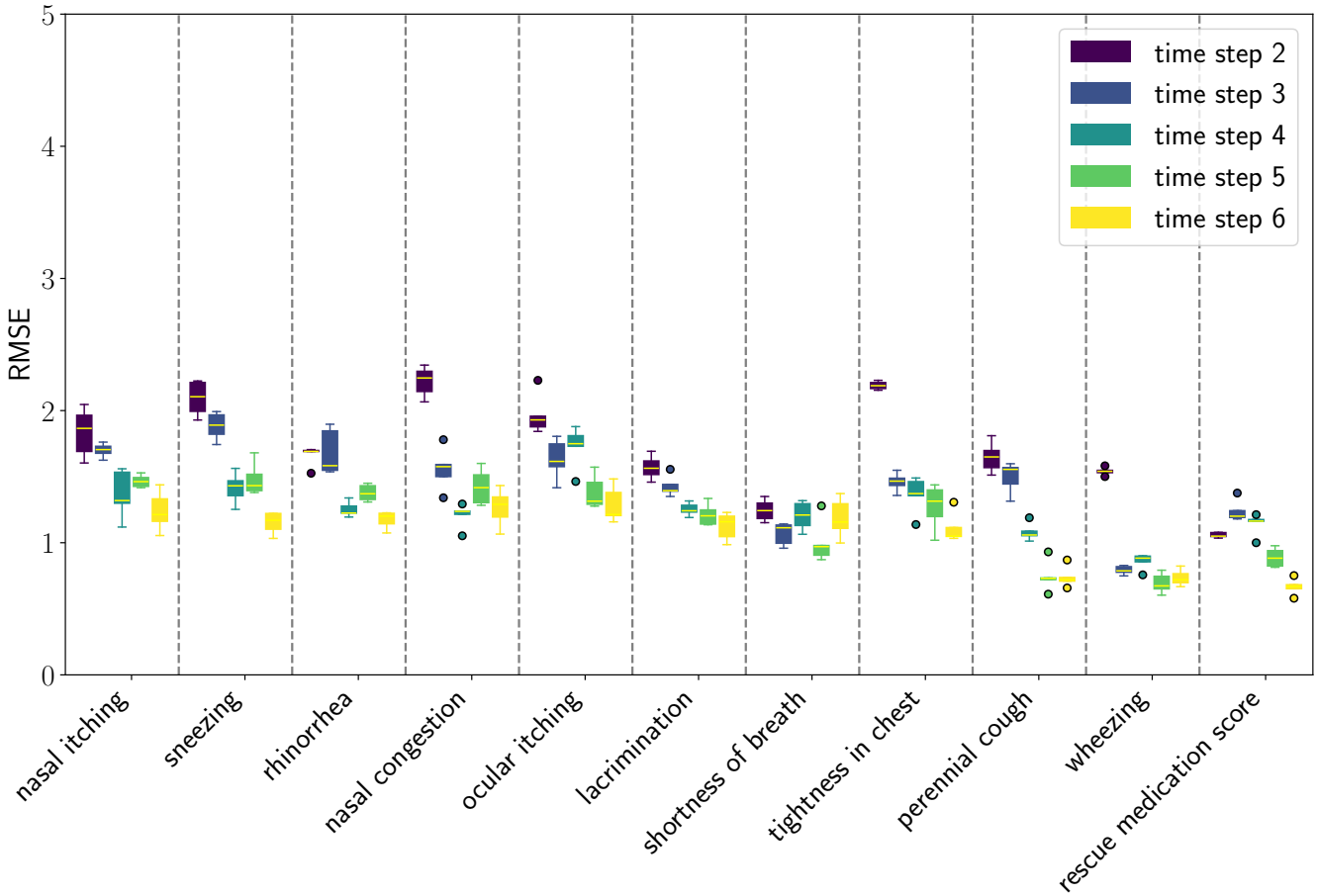


Figure 6. RMSE of LSTM one-step prediction across various scores and time steps.

4.2 Rollouts

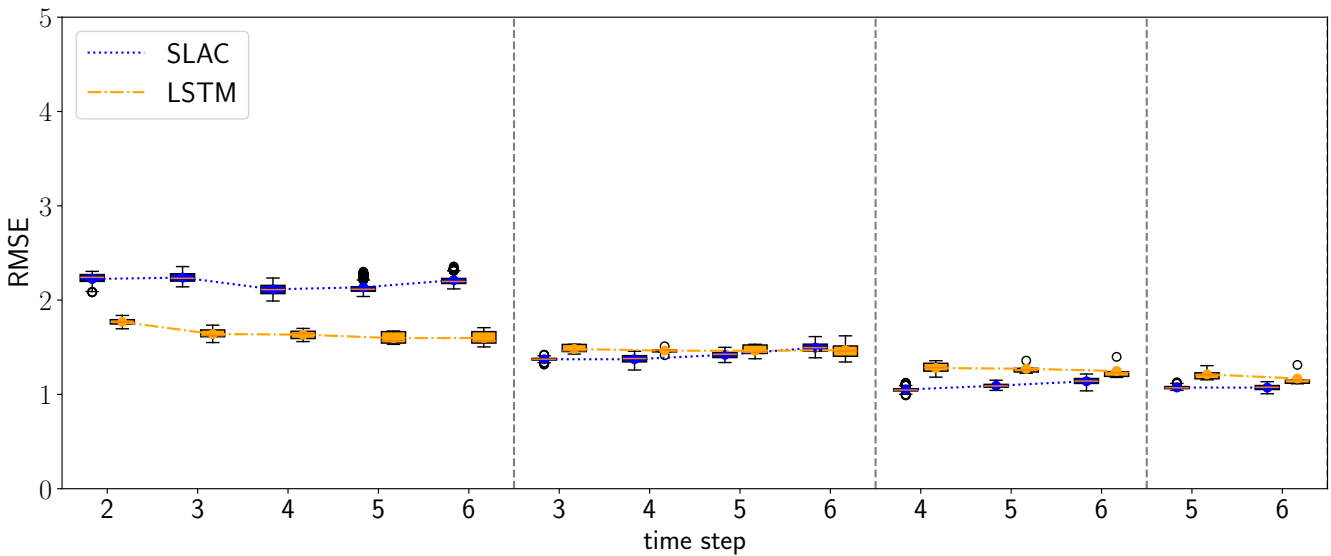


Figure 7. RMSE of the rollout prediction. The first time step in each subplot represents the beginning of the rollout time step.

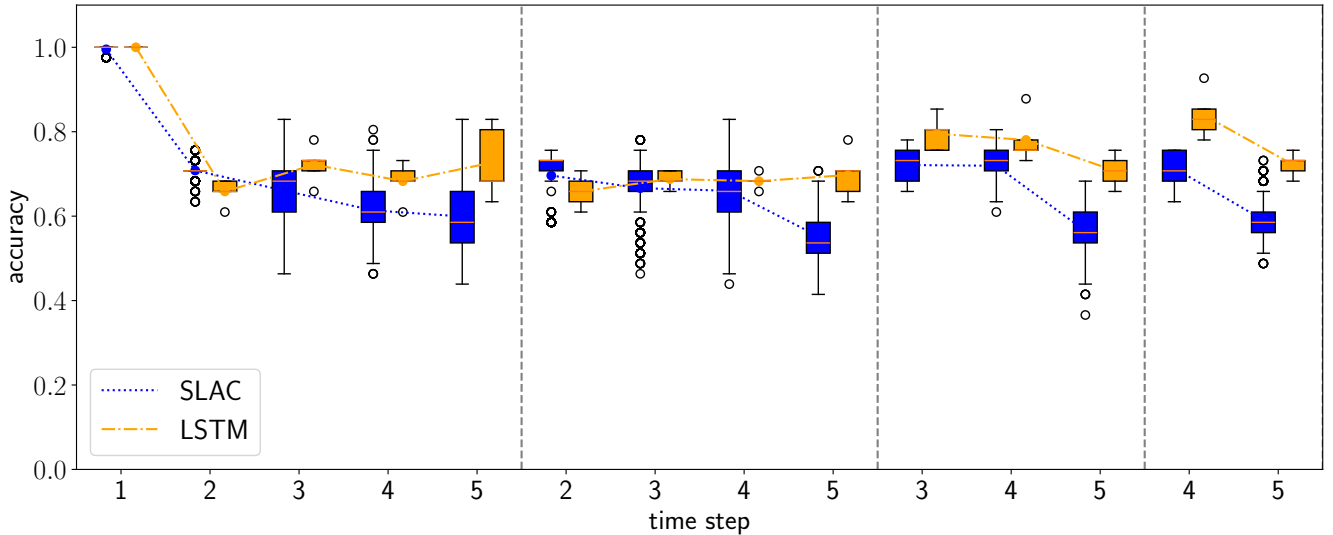


Figure 8. Accuracy of the rollout prediction. The first time step in each subplot represents the beginning of the rollout time step.

In the rollout experiment, our focus extends to a longer-term prediction. The SLAC prediction of $y_{t:T-1}$ and $x_{t+1:T}$ are computed based on $x_{1:t}$ and $a_{1:t-1}$. Actions, $\{a_i : i \geq t\}$ are inferred from the model’s output, y_t . Moreover, for time steps greater than t , we employ a prior in the latent space, which eliminates the need for the input of $x_{t:T}$. In the LSTM model, the predictions for $y_{t:T-1}$ and $x_{t+1:T}$ are based on $x_{1:t}$ and $y_{1:t-1}$.

Fig. 7 and 8 illustrate the performance of our model in multi-step predictions. Similar to one-step predictions, the accuracy generally improves with the availability of more information, except in the case of the adherence prediction at the fifth step. The results demonstrate the model’s proficiency in making long-term predictions.

4.3 Model as a simulator

Given the initial condition of a patient, we can assess the outcomes of various interventions. Clinically, if the patient’s adherence to treatment significantly impacts the prognosis (and there is a possibility of non-adherence), it becomes imperative for the doctor to emphasize treatment compliance. Conversely, if adherence makes little difference, it suggests the therapeutic approach may be ineffective for this patient, allowing the doctors to emphasize adherence efforts.

To evaluate the impact of varying actions on SLAC’s performance, we analyze how different actions affect the resulting scores. In the absence of a ground truth with diverse actions for the same patient, our focus shifts to examining whether the states are responsive to changes in actions. Considering initial states $x_{1:3}$ and actions $a_{1:2}$, we do rollouts with $a_{3:5}$, alternating between one and zero. This controlled alteration reveals that the average predicted value of x_6 under these conditions is -0.20 . This value is computed from the prediction outcomes for actions with ones minus those for actions with zeros. The result indicates that our model can be used as a simulator for doctors to see the impact of different treatments/therapies. Since the LSTM does not have similar functions (see Sec. 3.2.3), we only show the SLAC results.

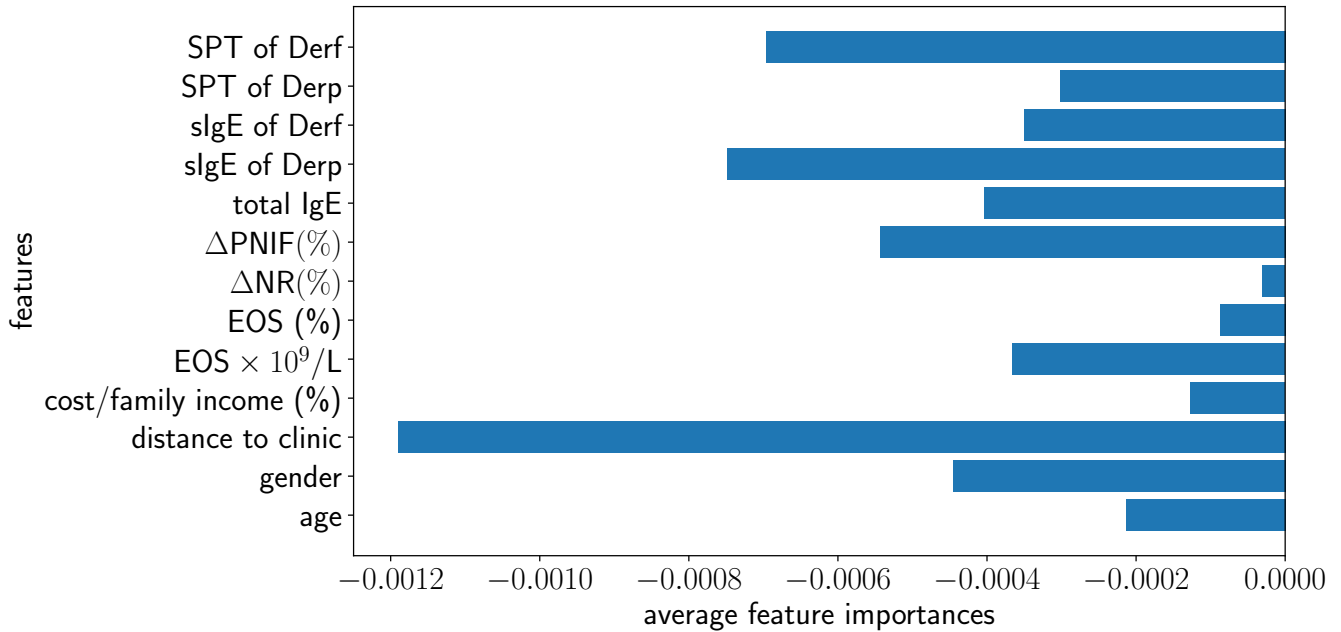


Figure 9. Importances of the factors.

4.4 Interpretability

Previous models and methods have been developed for interpreting machine learning algorithms, including SHAP (Lundberg and Lee, 2017) and Captum (Kokhlikyan et al., 2020). We opt for Captum, as it integrates more seamlessly with PyTorch-based code. Features with positive attributions positively influence a model’s prediction for a certain class, increasing its confidence in that prediction. We perform the measure of the factor importances using SLAC (see Fig. 9). The distance to the clinic significantly impacts patient adherence, especially if a patient is located far from the clinic or has relocated, as they are more likely to discontinue their visits. Following the distance, SPT of Derf and sIgE of Derf greatly influence the adherence. In contrast, Δ NR(%), EOS(%), and the cost/family income(%) have minimal impacts.

4.5 Architecture and computation

In this study, computational experiments were performed using an NVIDIA GeForce GTX 1080 Ti GPU, with the implementation done in PyTorch, version 2.1.0.

The SLAC model’s architecture featured 32 hidden dimensions each for variables z_1 and z_2 . Its encoder and decoder were symmetrically structured, each comprising five layers with 128 units. The primary activation function was LeakyReLU, set with a negative slope coefficient of 0.2. Both the encoder and decoder’s mean output layers were linear, while the STD layer utilized a Softplus activation. For binary classification tasks, a Sigmoid activation was used for output.

The LSTM architecture included a hidden dimension size of 128, with two LSTM layers. The output activation function for score prediction was linear, and like the SLAC model, a Sigmoid function was employed for binary classification outputs.

Both models shared the same optimization settings. They utilized the RAdam (Liu et al., 2019) optimizer with a learning rate of 0.001. The batch size was set at 64, and a gradient clipping value of 0.8 was applied

to ensure training stability. To prevent overfitting and enhance model generalization, a dropout rate of 0.05 was introduced. Additionally, both models incorporated Mixup as a data augmentation during training.

5 DISCUSSION

The reported adherence rates of SCIT ranged from around 23 % to 90 %, due to the non-uniform follow-up duration (2-4 years) (Passalacqua et al., 2013; Lee et al., 2019; Lemberg et al., 2017; Yang et al., 2018). Poor adherence in the three to five-year time span of AIT is an obstacle to reaching allergen tolerance and symptom remission. Recently proposed an ‘adherence and persistence in AIT (APAIT)’ checklist that assists researchers in assessing adherence or persistence to AIT in retrospective studies (Pfaar et al., 2023). The present study is the first research about the application of machine learning models in the adherence prediction of SCIT in AR patients. From our study, the accomplishment rate of the three-year treatment cycle was relatively low (35.4 %), while the rate of dropout after two years accounts for half (42.8 %) in the whole non-adherence cohort. Several researchers focus on these variables impacting the compliance of medical behaviors to enhance the intervention approach to reduce the withdrawal caused by disease-unrelated reasons. Even though the Covid-19 pandemic impacted the compliance of the majority of the patients in the three-year cycle, the first year since the pandemic’s outbreak appears to fundamentally built a barrier to patients, similar to the finding from Liu et al. (2021) that 11 % dropouts in the two years SCIT was observed caused by Covid-19. We excluded the patients who dropped out in the dose buildup phase within four months to minimize the dose-origin impact. Due to the uncovered cost from the public health care system and commercial insurance, financial burden accounts for a non-negligible factor in influencing the decision-making of patients. A similar finding from Lourenço et al. (2020). indicated that economic reasons contributed to the most frequent cause of SCIT cessation.

In comparison to the logistic regression analyses in the clinical field to identify independent predictors, the model from our study performed convincing interpretability. Previous research primarily concentrated on non-sequential prediction methods for adherence (Mousavi et al., 2022; Wang et al., 2020; Warren et al., 2022; Ruff et al., 2019). This approach presents a significant limitation in treatment processes, particularly for immunotherapy that often spans extended periods, such as three years. These non-sequential methods tend to predict only the overall outcome, overlooking the intricacies of intermediate time steps. To facilitate earlier intervention, a sequential model capable of making predictions at any given time step would be markedly more beneficial. While some subsequent studies have introduced sequential models (Hsu et al., 2022; Singh et al., 2022; Schleicher et al., 2023), their scope was restricted to predicting adherence alone. Our study enhances this approach by incorporating a state-action model, which can predict both adherence and score/state. This advancement allows for more precise and detailed analysis of patient cases by medical professionals.

Our study demonstrates notable findings in the domain of patient adherence prediction in subcutaneous immunotherapy. The comparison between the SLAC model and LSTM model reveals the distinct strengths and limitations of each approach. Notably, the SLAC exhibits greater flexibility, and it outperforms the LSTM in score prediction. This advantage likely stems from its ability to efficiently learn and generalize in complex environments, a trait that is crucial in medical data analysis. Conversely, the LSTM model shows better performance in predicting adherence, indicating its potential utility in scenarios where accurate forecasting of patient compliance is critical. Both models demonstrate the capability to handle longer sequences, extending beyond one-step prediction. This ability is crucial in medical settings where long-term patient monitoring and prediction are essential for effective treatment planning.

Overall, the study underscores the importance of selecting the appropriate model based on the specific requirements of the task, whether it be flexibility, precision in score prediction, or adherence prediction. The findings contribute to the growing field of machine learning applications in healthcare, particularly in enhancing patient-centered treatment strategies through accurate and personalized predictions. Future research could focus on evaluating the SLAC model's performance in simulating various actions, further enriching its applicability in clinical settings.

6 CONCLUSION

In summary, our study showcases the flexibility and score prediction superiority of the Sequential Latent Actor-Critic (SLAC) model, while highlighting the superior adherence prediction capabilities of the Long Short-Term Memory (LSTM) model. Both models demonstrate proficiency in managing extended sequence predictions, extending beyond single-step forecasts. This study emphasizes the utility and significance of selecting the appropriate model based on specific task requirements, be it for precision in score prediction or adherence forecasting. These findings make a substantial contribution to the application of machine learning in healthcare, particularly in improving patient-centered treatment strategies through accurate and tailored predictions.

CONFLICT OF INTEREST STATEMENT

The authors declare that the research was conducted in the absence of any commercial or financial relationships that could be construed as a potential conflict of interest.

DATA AVAILABILITY STATEMENT

The dataset for this study can be found in the [Subcutaneous-Immunotherapy-Dataset repository](#).

REFERENCES

- Alemi, A. A., Poole, B., Fischer, I., Dillon, J. V., Saourous, R. A., and Murphy, K. (2018). Fixing a broken ELBO. *ICML*
- Chen, N., Klushyn, A., Ferroni, F., Bayer, J., and Van Der Smagt, P. (2020). Learning flat latent manifolds with vaes. *ICML*
- Chen, N., van der Smagt, P., and Cseke, B. (2022). Local distance preserving auto-encoders using continuous knn graphs. In *Topological, Algebraic and Geometric Learning Workshops 2022*. 55–66
- Gregor, K., Papamakarios, G., Besse, F., Buesing, L., and Weber, T. (2018). Temporal difference variational auto-encoder. *arXiv preprint arXiv:1806.03107*
- Higgins, I., Matthey, L., Pal, A., Burgess, C., Glorot, X., Botvinick, M., et al. (2017). Beta-VAE: Learning basic visual concepts with a constrained variational framework. *ICLR*
- Hochreiter, S. and Schmidhuber, J. (1997). Long short-term memory. *Neural computation* 9, 1735–1780
- Hsu, W., Warren, J. R., and Riddle, P. J. (2022). Medication adherence prediction through temporal modelling in cardiovascular disease management. *BMC Medical Informatics and Decision Making* 22, 1–21
- Karl, M., Soelch, M., Bayer, J., and Van der Smagt, P. (2016). Deep variational bayes filters: Unsupervised learning of state space models from raw data. *arXiv preprint arXiv:1605.06432*

- Kingma, D. P., Salimans, T., Jozefowicz, R., Chen, X., Sutskever, I., and Welling, M. (2016). Improved variational inference with inverse autoregressive flow. *Advances in neural information processing systems* 29
- Kingma, D. P. and Welling, M. (2014). Auto-encoding variational Bayes. *ICML*
- Klushyn, A., Chen, N., Kurle, R., Cseke, B., and van der Smagt, P. (2019). Learning hierarchical priors in VAEs. *Advances in Neural Information Processing Systems* 32
- Kokhlikyan, N., Miglani, V., Martin, M., Wang, E., Alsallakh, B., Reynolds, J., et al. (2020). Captum: A unified and generic model interpretability library for pytorch. *arXiv preprint arXiv:2009.07896*
- Krishnan, R. G., Shalit, U., and Sontag, D. (2015). Deep kalman filters. *arXiv preprint arXiv:1511.05121*
- Lee, A. X., Nagabandi, A., Abbeel, P., and Levine, S. (2020). Stochastic latent actor-critic: Deep reinforcement learning with a latent variable model. *Advances in Neural Information Processing Systems* 33, 741–752
- Lee, J.-H., Lee, S.-H., Ban, G.-Y., Ye, Y.-M., Nahm, D.-H., Park, H.-S., et al. (2019). Factors associated with adherence to allergen specific subcutaneous immunotherapy. *Yonsei medical journal* 60, 570–577
- Lemberg, M.-L., Berk, T., Shah-Hosseini, K., Kasche, E.-M., and Mösges, R. (2017). Sublingual versus subcutaneous immunotherapy: patient adherence at a large german allergy center. *Patient preference and adherence* , 63–70
- Liu, J., Feng, X., Wang, H., and Yu, H. (2021). Compliance with subcutaneous immunotherapy and factors affecting compliance among patients with allergic rhinitis. *American Journal of Otolaryngology* 42, 103125
- Liu, L., Jiang, H., He, P., Chen, W., Liu, X., Gao, J., et al. (2019). On the variance of the adaptive learning rate and beyond. *arXiv preprint arXiv:1908.03265*
- Lourenço, T., Fernandes, M., Coutinho, C., Lopes, A., Spinola Santos, A., Neto, M., et al. (2020). Subcutaneous immunotherapy with aeroallergens-evaluation of adherence in real life
- Lundberg, S. M. and Lee, S.-I. (2017). A unified approach to interpreting model predictions. *Advances in neural information processing systems* 30
- Meltzer, E. O. (2016). Allergic rhinitis: burden of illness, quality of life, comorbidities, and control. *Immunology and Allergy Clinics* 36, 235–248
- Mousavi, H., Karandish, M., Jamshidnezhad, A., and Hadianfard, A. M. (2022). Determining the effective factors in predicting diet adherence using an intelligent model. *Scientific Reports* 12, 12340
- Organization, W. H. et al. (2003). *Adherence to long-term therapies: evidence for action* (World Health Organization)
- Passalacqua, G., Baiardini, I., Senna, G., and Canonica, G. (2013). Adherence to pharmacological treatment and specific immunotherapy in allergic rhinitis. *Clinical & Experimental Allergy* 43, 22–28
- Pfaar, O., Devillier, P., Schmitt, J., Demoly, P., Hilberg, O., DuBuske, L., et al. (2023). Adherence and persistence in allergen immunotherapy (apait): A reporting checklist for retrospective studies. *Allergy*
- Rezende, D. J., Mohamed, S., and Wierstra, D. (2014). Stochastic backpropagation and approximate inference in deep generative models. In *ICML*. vol. 32, 1278–1286
- Rezende, D. J. and Viola, F. (2018). Taming VAEs. *CoRR*
- Roberts, G., Pfaar, O., Akdis, C., Ansotegui, I., Durham, S., Gerth van Wijk, R., et al. (2018). Eacii guidelines on allergen immunotherapy: allergic rhinoconjunctivitis. *Allergy* 73, 765–798
- Ruff, C., Koukalova, L., Haefeli, W. E., and Meid, A. D. (2019). The role of adherence thresholds for development and performance aspects of a prediction model for direct oral anticoagulation adherence. *Frontiers in Pharmacology* 10, 113

- Schleicher, M., Unnikrishnan, V., Pryss, R., Schobel, J., Schlee, W., and Spiliopoulou, M. (2023). Prediction meets time series with gaps: User clusters with specific usage behavior patterns. *Artificial Intelligence in Medicine* 142, 102575
- Singh, A., Chakraborty, S., He, Z., Tian, S., Zhang, S., Lustria, M. L. A., et al. (2022). Deep learning-based predictions of older adults' adherence to cognitive training to support training efficacy. *Frontiers in Psychology* 13, 980778
- Sønderby, T., C. K. and Raiko, Maaløe, L., Sønderby, S. K., and Winther, O. (2016). Ladder variational autoencoders. *NeurIPS*
- Srivastava, N., Hinton, G., Krizhevsky, A., Sutskever, I., and Salakhutdinov, R. (2014). Dropout: a simple way to prevent neural networks from overfitting. *The journal of machine learning research* 15, 1929–1958
- Wang, L., Fan, R., Zhang, C., Hong, L., Zhang, T., Chen, Y., et al. (2020). Applying machine learning models to predict medication nonadherence in crohn's disease maintenance therapy. *Patient preference and adherence* , 917–926
- Warren, D., Marashi, A., Siddiqui, A., Eijaz, A. A., Pradhan, P., Lim, D., et al. (2022). Using machine learning to study the effect of medication adherence in opioid use disorder. *PLoS One* 17, e0278988
- Yang, Y., Wang, Y., Yang, L., Wang, J., Huang, N., Wang, X., et al. (2018). Risk factors and strategies in nonadherence with subcutaneous immunotherapy: a real-life study. In *International Forum of Allergy & Rhinology* (Wiley Online Library), vol. 8, 1267–1273
- Zhang, H., Cisse, M., Dauphin, Y. N., and Lopez-Paz, D. (2017). mixup: Beyond empirical risk minimization. *arXiv preprint arXiv:1710.09412*